



UNIVERSITÉ DE
MONTPELLIER

MIMESIS

**ϕ -FEM-FNO: A NEW APPROACH TO TRAIN A NEURAL OPERATOR
AS A FAST PDE SOLVER FOR VARIABLE GEOMETRIES.**

04/06/2024

ECCOMAS 2024, Lisbon

Michel Duprez¹, Vanessa Lleras², Alexei Lozinski³, Vincent Vignon⁴
and Killian Vuillemot^{1,2}

¹Inria, Strasbourg, France, ²IMAG, Montpellier, France,
³LMB, Besançon, France, ⁴IRMA, Strasbourg, France.

① Motivation

② The ϕ -FEM technique

③ ϕ -FEM and Neural networks

④ Conclusion

① Motivation

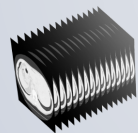
② The ϕ -FEM technique

③ ϕ -FEM and Neural networks

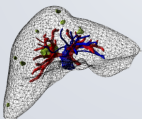
④ Conclusion

Objectives

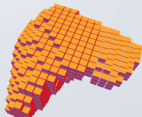
Develop **real-time, patient specific digital twins** for computer-aided surgical interventions.



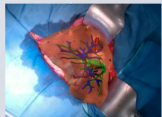
① Image



② 3D reconstruction



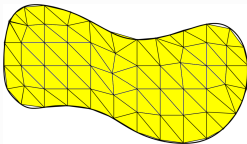
③ Numerical method



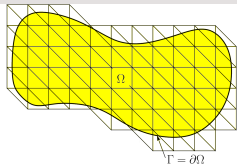
④ Surgical navigation

- ▶ Simulation of the deformations of organs : PDEs → FEMs,
- ▶ Complex geometries → Unfitted FEMs,
- ▶ Real-time constructions → machine learning techniques.

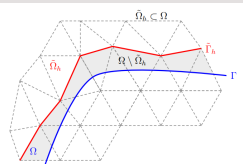
VERY SHORT STORY OF FEMs



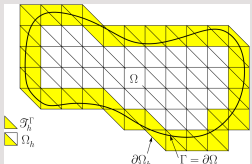
(a) Standard FEM (Clough 60s).



(b) XFEM (Moes and al., 2006)
→ Non-classical shape functions,
CutFEM (Burman, Hansbo, 2010-2014)
→ cut cells and partial integrals.



(c) Shifted Boundary method (Main, Scovazzi, 2017)
→ Taylor development near the boundary.



(d) ϕ -FEM (Duprez and Lozinski, 2020)
→ Level-set function

Problems on complex shapes → unfitted FEMs

① Motivation

② The ϕ -FEM technique

③ ϕ -FEM and Neural networks

④ Conclusion

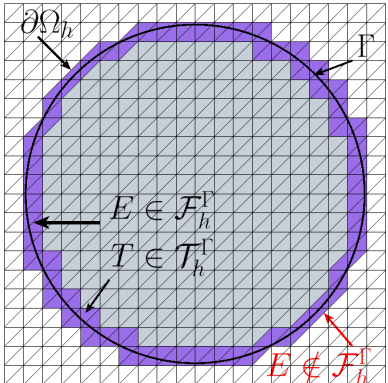
THE IDEA OF ϕ -FEM

Level-set function

$$\Omega = \{\phi < 0\} \text{ and } \Gamma = \{\phi = 0\}.$$

The spaces

- ▶ \mathcal{T}_h : ϕ -FEM mesh,
- ▶ \mathcal{T}_h^Γ : cells of \mathcal{T}_h cut by the boundary (purple triangles),
- ▶ \mathcal{F}_h^Γ : internal facets of \mathcal{T}_h^Γ .



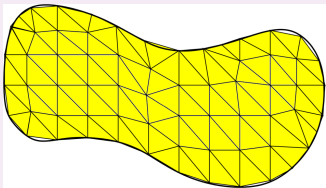
Example with $\phi(x, y) = -1 + x^2 + y^2$.

Example (Poisson-Dirichlet equation)

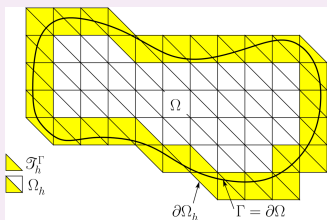
$$-\Delta u = f \quad \text{in } \Omega, \quad u = g \quad \text{on } \Gamma.$$

Standard FEM

Find u s.t. $\begin{cases} -\Delta u = f, & \text{in } \Omega, \\ u = g, & \text{on } \Gamma. \end{cases}$

 **ϕ -FEM**

Find w s.t. $\begin{cases} -\Delta u = f, & \text{in } \Omega_h, \\ u = \phi w + g, & \text{in } \Omega_h. \end{cases}$



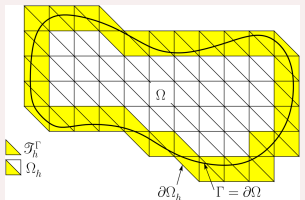
Example (Poisson-Dirichlet equation)

$$-\Delta u = f \quad \text{in } \Omega, \quad u = g \quad \text{on } \Gamma.$$

ϕ -FEM scheme

Find w_h such that for all v_h ,

$$\begin{aligned} & \int_{\Omega_h} \nabla(\phi_h w_h + g_h) \cdot \nabla(\phi_h v_h) \\ & - \int_{\partial\Omega_h} \frac{\partial}{\partial n} (\phi_h w_h + g_h) \phi_h v_h \\ & + \boxed{\text{stabs}} = \int_{\Omega_h} f_h \phi_h v_h - \boxed{\text{stabs}}. \end{aligned}$$



Who are «stabs»?

- ▶ First order : Ghost penalty (\mathcal{S}_1),
- ▶ Second order : least square imposition of the strong formulation on \mathcal{T}_h^Γ (\mathcal{S}_2).

$$\int_{\Omega_h} \nabla(\phi_h w_h + g_h) \cdot \nabla(\phi_h v_h) - \int_{\partial\Omega_h} \frac{\partial}{\partial n}(\phi_h w_h + g_h) \phi_h v_h \\ + \sigma h \underbrace{\sum_{E \in \mathcal{F}_\Gamma} \int_E \left[\frac{\partial}{\partial n}(\phi_h w_h + g_h) \right] \left[\frac{\partial}{\partial n}(\phi_h v_h) \right]}_{(\mathcal{S}_1) : \text{Ghost penalty, jump over the facets}}$$

$$+ \sigma h^2 \underbrace{\sum_{T \in \mathcal{T}_h^\Gamma} \int_T \Delta(\phi_h w_h + g_h) \Delta(\phi_h w_h)}_{(\mathcal{S}_2) : \text{least square imposition of the governing equation}} = \int_{\Omega_h} f_h \phi_h v_h$$

$$\underbrace{-\sigma h^2 \sum_{T \in \mathcal{T}_h^\Gamma} \int_T f \Delta(\phi_h w_h)}_{\mathcal{S}_2 \text{'s friend}} .$$

Interests of the method

- ▶ Optimal convergence in L^2 and H^1 norms,
- ▶ **Easy to implement**: standard shape functions, no cut cells —> standard quadrature rules,
- ▶ Acceptable conditioning of the finite element matrix,
- ▶ **No need to generate a conforming mesh.**

Other schemes

- ▶ Dirichlet or Neumann boundary conditions,
- ▶ Linear elasticity problems,
- ▶ Stokes problem,
- ▶ Heat equation.

① Motivation

② The ϕ -FEM technique

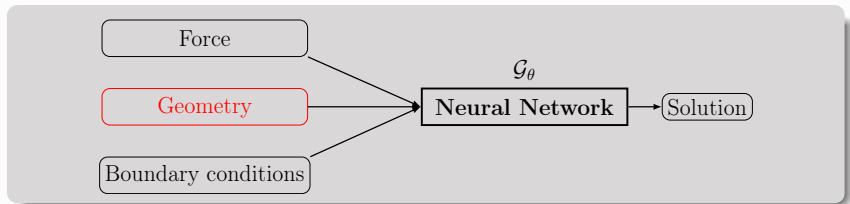
③ ϕ -FEM and Neural networks

④ Conclusion

OUR FRAMEWORK

In the context of real-time simulations, we need
quasi-instantaneous results.

- ▶ ϕ -FEM : precise but slow → Not real-time
- ▶ Neural Networks → Real time
- ▶ ϕ -FEM + Neural Networks → Precise and real-time method?

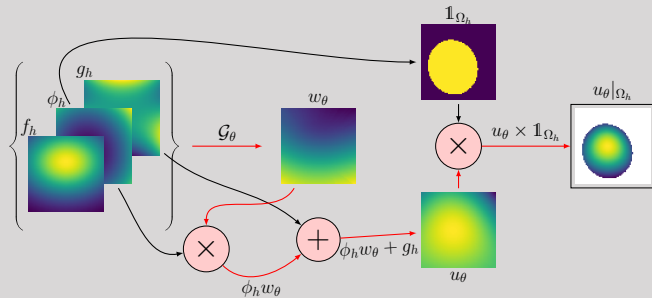


OUR FRAMEWORK

In the context of real-time simulations, we need
quasi-instantaneous results.

- ▶ ϕ -FEM : precise but slow → Not real-time
- ▶ Neural Networks → Real time
- ▶ ϕ -FEM + Neural Networks → Precise and real-time method?

The idea : construct an operator \mathcal{G}_θ



How to combine ϕ -FEM and neural networks to obtain fast and precise results?

→ the Fourier Neural Operator.

Why choose the FNO?

- ▶ Neural operator : learns a mapping, not a solution,
- ▶ Uses FFT → requires Cartesian grid, as ϕ -FEM does,
- ▶ According to the authors, more accurate than other ML-methods :

	NN	PCANN	DeepOnet	GNO	LNO	FNO
Darcy Flow	0.17	0.02	0.04	0.03	0.05	0.01
1D Burgers	0.47	0.04	0.06	0.06	0.02	0.001

L^2 errors of different methods [Kovachki et al, 2023].

- ▶ Almost no need to change the underlying architecture when changing the governing PDE.

WHAT IS THE FNO? (I)

Parametric application :

$$\mathcal{G}_\theta : \mathbb{R}^{n_x \times n_y \times 3} \xrightarrow{N} \mathbb{R}^{n_x \times n_y \times 3} \xrightarrow{P_\theta} \mathbb{R}^{n_x \times n_y \times n_d} \xrightarrow{\mathcal{H}_\theta^1} \mathbb{R}^{n_x \times n_y \times n_d} \xrightarrow{\mathcal{H}_\theta^2} \dots \xrightarrow{\mathcal{H}_\theta^4} \mathbb{R}^{n_x \times n_y \times n_d} \xrightarrow{Q_\theta} \mathbb{R}^{n_x \times n_y \times 1} \xrightarrow{N^{-1}} \mathbb{R}^{n_x \times n_y \times 1}.$$

- ▶ In and out dimensions : $X = (f_h, \phi_h, g_h) \rightarrow w_h$, with f_h, ϕ_h, g_h and w_h images of shape (n_x, n_y) .
- ▶ N and N^{-1} : standardization and unstandardization (channel by channel),
- ▶ P_θ and Q_θ : «embedding and projection»,

$$P_\theta(X)_{ijk} = \sum_{k'=1}^3 W_{kk'}^{P_\theta} X_{ijk'} + B_k^{P_\theta} \in \mathbb{R}^{n_d},$$

→ from original dimension 3 to «hidden dimension», $n_d >> 3$.

$$Q_\theta(X)_{ij} = \left[\sum_{k=1}^{n_Q} W_{1k}^{Q_\theta,2} \sigma \left(\sum_{k'=1}^{n_d} W_{kk'}^{Q_\theta,1} X_{ijk'} + B_k^{Q_\theta,1} \right) \right] + B^{Q_\theta,2} \in \mathbb{R}$$

→ from «hidden dimension» n_d to final dimension 1.

WHAT IS THE FNO? (II)

Parametric application :

$$\mathcal{G}_\theta : \mathbb{R}^{n_x \times n_y \times 3} \xrightarrow{N} \mathbb{R}^{n_x \times n_y \times 3} \xrightarrow{P_\theta} \mathbb{R}^{n_x \times n_y \times n_d} \xrightarrow{\mathcal{H}_\theta^1} \mathbb{R}^{n_x \times n_y \times n_d} \xrightarrow{\mathcal{H}_\theta^2} \dots \xrightarrow{\mathcal{H}_\theta^4} \mathbb{R}^{n_x \times n_y \times n_d} \xrightarrow{Q_\theta} \mathbb{R}^{n_x \times n_y \times 1} \xrightarrow{N^{-1}} \mathbb{R}^{n_x \times n_y \times 1}.$$

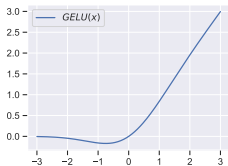
Each layer \mathcal{H}_θ^ℓ is defined by :

$$\mathcal{H}_\theta^\ell = \sigma \left(\mathcal{C}_\theta^\ell(X) + \mathcal{B}_\theta^\ell(X) \right)$$

\downarrow
 $\mathcal{F}^{-1} \left(W^{\mathcal{C}_\theta^\ell} \mathcal{F}(X) \right)$

with \mathcal{F} the real-FFT and
 \mathcal{F}^{-1} its inverse.

\downarrow
 $\mathcal{B}_\theta^\ell(X)_{ijk}$
 $= \sum_{k'=1}^{n_d} W_{kk'}^{\mathcal{B}_\theta^\ell} X_{ijk'} + B_k^{\mathcal{B}_\theta^\ell}$



The coefficients of $W^{\mathcal{C}_\theta^\ell}$ are complex trainable parameters.

The coefficients of $W^{\mathcal{B}_\theta^\ell}$ and $B_\theta^{\mathcal{B}_\theta^\ell}$ are real trainable parameters.

WHAT IS THE FNO? (III)

Question :

How many trainable parameters for ϕ -FEM-FNO?

$$\mathcal{C}_\theta^l : 2 \times \underbrace{n_d}_{\substack{\text{Number of in channels} \\ \text{Number of out channels}}} \times \underbrace{n_d}_{\substack{\text{Number of in channels} \\ \text{Number of out channels}}} \times \underbrace{m_x \times m_y}_{\text{Number of Fourier modes}}$$

- ▶ $\mathcal{F}(X)$: RFFT \rightarrow low frequencies stored in NW and SW corners,
- ▶ High frequencies negligible $\implies W = 0$ outside NW and SW corners,
- ▶ Size of the corners = «number of modes» = m_x, m_y ,
- ▶ Finally, for each corner : $n_d \times n_d \times m_x \times m_y$ parameters $\longrightarrow \times 2$.

Total number :

$$P_\theta : \underbrace{3 \times n_d + n_d}_{4 \times n_d} + 4 \times \underbrace{(2 \times n_d^2 \times m_x \times m_y + n_d^2 + n_d)}_{\mathcal{H}_\theta^l} + \underbrace{B_\theta^l}_{\substack{\text{C_θ^l : by truncation of} \\ \text{high frequencies}}} + \underbrace{Q_\theta : n_d \times n_Q + n_Q + n_Q \times 1 + 1}_{(n_d + 2) \times n_Q + 1} .$$

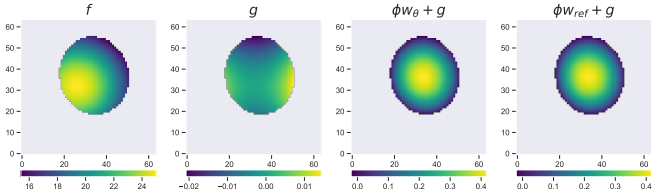
Does not depend on the resolution of the images!

First test case

$$-\Delta u = f, \text{ in } \Omega, \quad u = g, \text{ on } \Gamma,$$

- ▶ Ω is a random rotated ellipse defined using the signed distance ϕ ,
- ▶ f is a random gaussian force centered in Ω with constant amplitude
 $\implies f \in [0, 25],$
- ▶ $g_{(\alpha, \beta)}(x, y) = \alpha ((x - 0.5)^2 - (y - 0.5)^2) \cos(\beta y \pi)$
 $\implies g \in [-0.17, 0.15],$
- ▶ $\implies u \in [-0.17, 0.87].$

Dataset : 1500 training data, 300 validation data.

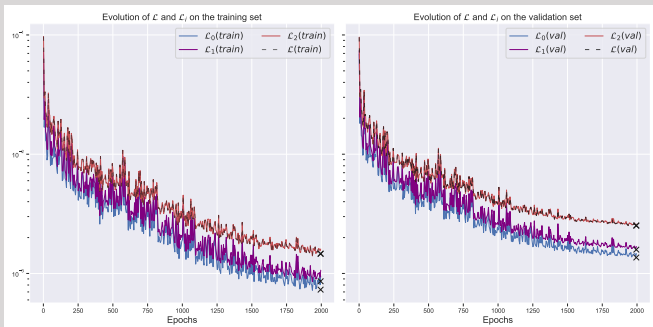


First test case

$$-\Delta u = f, \text{ in } \Omega, \quad u = g, \text{ on } \Gamma,$$

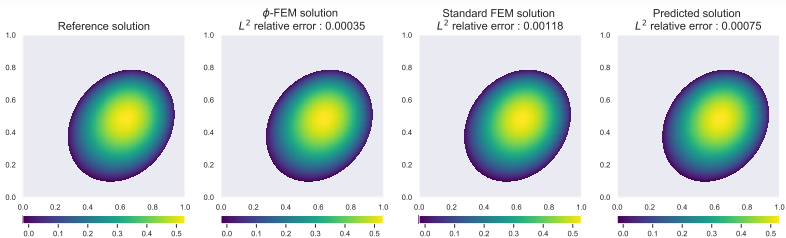
where Ω is a random rotated ellipse.

Convergence of the loss function : $\approx \|\cdot\|_{2,\Omega_h}$

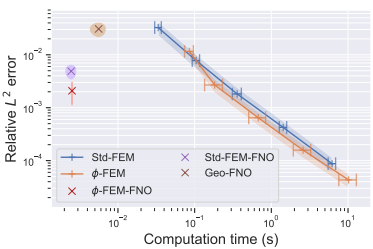
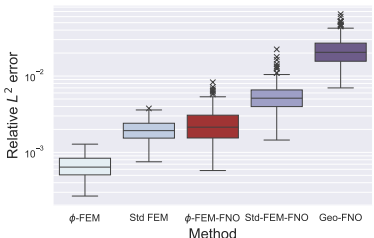


ϕ -FEM-FNO VS OTHER TECHNIQUES

15



Outputs of the first three methods.



Errors of the methods.

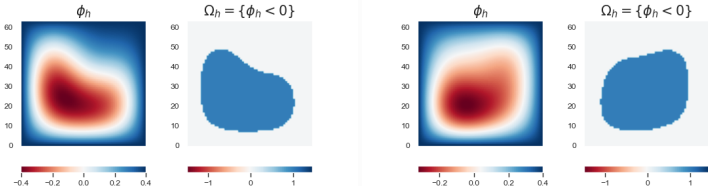
Second test case

$$-\Delta u = f, \text{ in } \Omega, \quad u = g, \text{ on } \Gamma,$$

where Ω is defined using Fourier series,

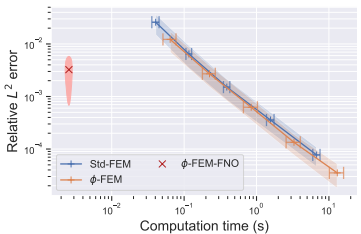
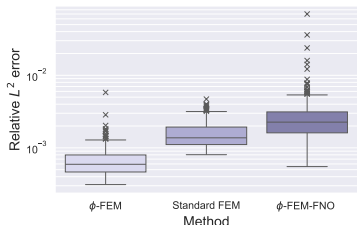
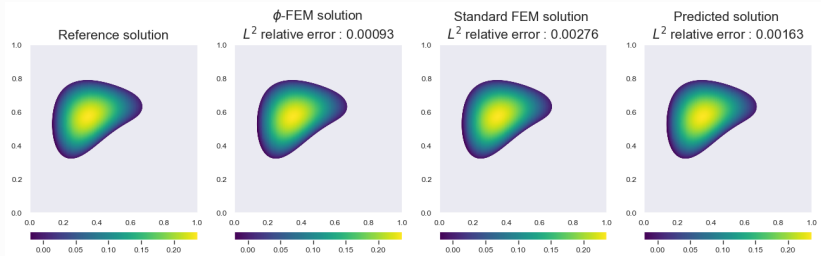
$$\phi(x, y) = 0.4 - \sum_{k=1}^3 \sum_{l=1}^3 \alpha_{kl} \sin(k\pi x) \sin(l\pi y),$$

Dataset : 2200 training data, 467 validation data.



Examples of level-set functions and corresponding domains.

ϕ -FEM AND FNO : COMPLEX SHAPES



① Motivation

② The ϕ -FEM technique

③ ϕ -FEM and Neural networks

④ Conclusion

Results

- ▶ Real-time : ≈ 100 times faster than FEM solvers,
- ▶ ≈ 5 times faster and more precise than the previous work Geo-FNO.

Perspectives :

- ▶ More realistic test cases,
- ▶ Mixed Dirichlet-Neumann boundary conditions, Time-Dependant PDE's, Linear and non-linear elasticity, ...
- ▶ 3D problems,
- ▶ Validation on organ geometries.

- ▶ 05/06/2024, 10 :30 - 12 :30, MS064B —→ **A. Lozinski** (Keynote Lecture) :
« ϕ -FEM : a fictitious domain finite element method on geometries defined by level-sets»;
- ▶ 06/06/2024, 10 :30 - 12 :30, MS064E —→ **M. Duprez** :
«A finite difference scheme with an optimal convergence for elliptic PDEs on domains defined by a level-set function»;
- ▶ 06/06/2024, 14 :30 - 16 :30, MS061B —→ **V. Lleras** :
«A new immersed boundary method (ϕ -FEM) to treat Stokes equations and particulate ows».

Thank you for your attention!

- ▶ The standardization and unstandardization operators are applied channel by channel and are given by :

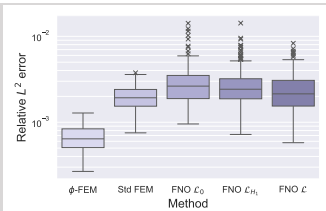
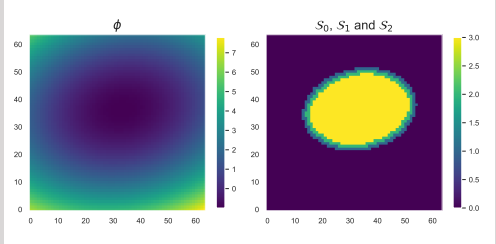
$$C^N = N(C) = \left(\frac{C - \text{mean}(C^{\text{train}})}{\text{std}(C^{\text{train}})} \right), \quad (N)$$

$$N^{-1}(Y) = Y \times \text{std}(Y^{\text{train}}) + \text{mean}(Y^{\text{train}}). \quad (N^{-1})$$

WHAT CHOICE FOR THE LOSS \mathcal{L} ?

$$H^2 \text{ norm : } \mathcal{L}^2 \approx \|\cdot\|_{0,\mathcal{S}_0}^2 + |\cdot|_{1,\mathcal{S}_1}^2 + |\cdot|_{2,\mathcal{S}_2}^2$$

- ▶ First and second derivatives : finite differences.
- ▶ Need to reduce the computational domain :



THE LOSS FUNCTION

$$\mathcal{L}(U_{\text{true}}; U_{\theta}) = \frac{1}{N_{\text{data}}} \sum_{n=0}^{N_{\text{data}}} \sqrt{\frac{\sum_{i=0}^2 \mathcal{E}_i(u_{\text{true}}^n; u_{\theta}^n)}{\sum_{i=0}^2 \mathcal{N}_i(u_{\text{true}}^n)}},$$

where

$$\mathcal{E}_0(u_{\text{true}}^n; u_{\theta}^n) = \sum_{\mathcal{S}_0} \|u_{\text{true}}^n(i, j) - u_{\theta}^n(i, j)\|^2,$$

$$\mathcal{E}_1(u_{\text{true}}^n; u_{\theta}^n) = \sum_{\mathcal{S}_1} \left(\|\nabla_x^h u_{\text{true}}^n(i, j) - \nabla_x^h u_{\theta}^n(i, j)\|^2 + \|\nabla_y^h u_{\text{true}}^n(i, j) - \nabla_y^h u_{\theta}^n(i, j)\|^2 \right),$$

$$\mathcal{E}_2(u_{\text{true}}^n; u_{\theta}^n) = \sum_{\mathcal{S}_2} \left(\|\nabla_x^h \nabla_x^h u_{\text{true}}^n(i, j) - \nabla_x^h \nabla_x^h u_{\theta}^n(i, j)\|^2 \right.$$

$$\left. + \|\nabla_x^h \nabla_y^h u_{\text{true}}^n(i, j) - \nabla_x^h \nabla_y^h u_{\theta}^n(i, j)\|^2 + \|\nabla_y^h \nabla_x^h u_{\text{true}}^n(i, j) - \nabla_y^h \nabla_x^h u_{\theta}^n(i, j)\|^2 + \|\nabla_y^h \nabla_y^h u_{\text{true}}^n(i, j) - \nabla_y^h \nabla_y^h u_{\theta}^n(i, j)\|^2 \right),$$

and

$$\mathcal{N}_0(u_{\text{true}}^n) = \sum_{\mathcal{S}_0} \|u_{\text{true}}^n(i, j)\|^2,$$

$$\mathcal{N}_1(u_{\text{true}}^n) = \sum_{\mathcal{S}_1} \left(\|\nabla_x^h u_{\text{true}}^n(i, j)\|^2 + \|\nabla_y^h u_{\text{true}}^n(i, j)\|^2 \right),$$

$$\mathcal{N}_2(u_{\text{true}}^n) = \sum_{\mathcal{S}_2} \left(\|\nabla_x^h \nabla_x^h u_{\text{true}}^n(i, j)\|^2 + \|\nabla_x^h \nabla_y^h u_{\text{true}}^n(i, j)\|^2 + \|\nabla_y^h \nabla_x^h u_{\text{true}}^n(i, j)\|^2 + \|\nabla_y^h \nabla_y^h u_{\text{true}}^n(i, j)\|^2 \right).$$